4. R. P. Manohar and S. R. K. Iyengar, Transient heat transfer to a droplet suspended in an electric field, *Numer. Heat Transfer* **14**, 499–510 (1988).

5. R. Kronig and J. C. Brink, On the theory of extraction from falling droplets, *Appl. Sci. Res.* **A2**, 142–154 (1950).

Int. J. Heat Mass Transfer. Vol. 36, No. 12, pp. 3155–3158, 1993
Printed in Great Britain

0017-9310/93 $6.00 + 0.00

A close upper bound for the conduction shape factor of a uniform thickness, 2D layer

A. V. HASSANI
National Renewable Energy Laboratory, Thermal Sciences and Engineering Branch, Building Energy Technology Program, Golden, Colorado 80401, U.S.A.

and

K. G. T. HOLLANDS and G. D. RAITHBY
Mechanical Engineering Department, University of Waterloo, Waterloo, Ontario N2L 3G1, Canada

(*Received* 11 *May* 1992 *and in final form* 7 *December* 1992)

INTRODUCTION

THE HEAT transfer by conduction through layers of uniform thickness surrounding a planar wall, a sphere, or a circular cylinder can be found from simple solutions to the one-dimensional conduction equation. Simple exact solutions are not available, however, when the uniform layer surrounds other body shapes. Yet in practice, it is often desirable to predict the heat transfer through such layers—for example, through layers of insulation applied to diverse objects, such as ducts, which come in a variety of cross-sectional shapes. Calculating natural convection heat transfer by the 'conduction layer method' (Raithby and Hollands [1]) provides yet another circumstance in which one needs to predict heat conducted through a uniform layer. The 'conduction layer method' provides its answer in terms of the thickness of a hypothetical stagnant fluid layer offering the same resistance to heat transfer as the actual boundary layer; finding the heat transfer then requires solving for the heat conducted through this layer.

Finding the heat transfer reduces to finding the layer's thermal resistance R, or equivalently the shape factor, S, where

$$S = \frac{1}{kR} = \frac{Q}{k\Delta T} \tag{1}$$

where Q is the heat transfer, ΔT is the applied temperature difference, and k is the thermal conductivity of the layer material. The present paper derives a simple approximate equation for S for cases in which the flow of heat is two-dimensional. The equation gives an upper bound for the exact value of S. The closeness of the upper bound to the exact solution and the extreme simplicity of the result make this approximate solution of practical interest.

Previous related works (Smith *et al.* [2], Balcerzak and Rayner [3], Lewis [4], Dungan [5], Laura and Susemihl [6], Laura and Sanchez Sarmiento [7, 14] and Simeza and Yovanovich [8]) all considered layers of non-uniform thickness and therefore do not strictly apply to the uniform layer problem.

To better define the problem, we first note that in the cross-sectional view (Fig. 1(a)), the layer lies between two closed curves: an inner curve C_i, and an outer curve C_o, which is spaced uniformly at perpendicular distance B from C_i. Thus curve C_o is defined as the locus of points traced by constructing outward normals to C_i and measuring out distance B along the normal. Sharp vertices in C_i that occur, for example, when C_i is a polygon (Fig. 1(b)), would appear to leave C_o undefined by this construction process, over the region near the vertex. But if we consider the vertex as a limiting case of a small circular arc near the vertex, we find that, C_o is simply filled in by an arc of radius B centered at the vertex (Fig. 1(c)).

If B is sufficiently large, and C_i is concave over parts of its length, the curve C_o may be found to be self-intersecting (Fig. 1(d)). This can happen only on concave regions of C_i; it occurs if a local radius of curvature is less than B. (Vertices having internal angles, ϕ, greater than π will always produce self-intersection of C_o, regardless of B.) If C_o self-intersects, one can question whether it is possible to actually produce a uniform layer surrounding the cylinder. Thus we exclude from the purview of the paper those combinations of B and C_i that produce self-intersection of C_o.

The present paper's derivation of an equation for S draws upon the observation of Elrod [9] that the value of S will be no greater than that derived when the shapes of the isotherms are arbitrarily assumed. The closer the assumed shapes are to those of the true isotherms, the more accurate will be the derived value of S. It happens that one particular set of assumed shapes for the isotherms satisfies many of the requirements for the true isotherm shapes and yields a very simple, general-purpose expression for the corresponding derived values of S. These particular assumed shapes are curves constructed identically to those used to construct C_o, but spaced arbitrary distance u, rather than B, from C_i, with $0 \leqslant u \leqslant B$. In this paper, the equation for S derived from this model is tested against exact results for some special cases chosen to be the most demanding on the model.

ANALYSIS

Properties of curves C_u

Let a curve constructed at constant perpendicular distance u from C_i be denoted by C_u. We first show that

$$P_u = P_i + 2\pi u \tag{2}$$

where P_i and P_u are the lengths (or perimeters) of C_i and C_u, respectively. We also show that any normal to C_i, when extended to C_u as a straight line, meets C_u at right angles. To derive these results for a smooth curve, we let $\mathbf{r}_u$ and $\mathbf{r}_i$ represent the position vectors of various points on curves C_u and C_i, respectively, as shown in Fig. 2. Then

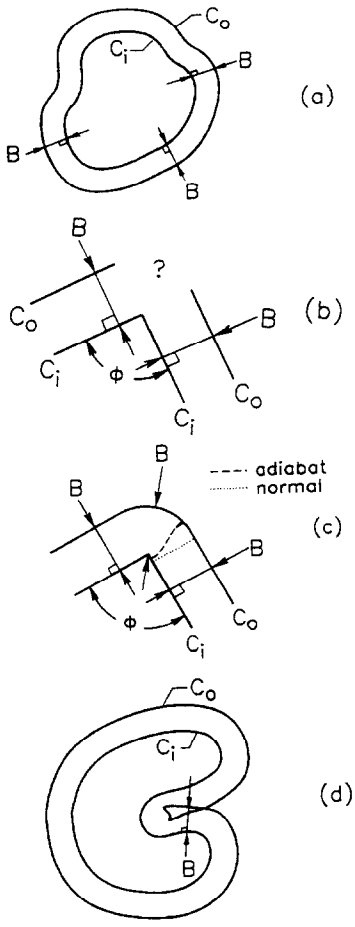

FIG. 1. Sketches of some possible curves C_i and C_o forming the bounds of the layer of uniform perpendicular thickness B between two given cylinders. (a) For a given C_i, C_o is generated by everywhere on C_i measuring distance B out from C_i. (b) If C_i has a sharp corner, C_o is undefined over a certain region. (c) This problem is overcome by filling in with a circular arc of radius B. (d) In some instances the C_o so generated is found to be self-intersecting; these situations are not treated by the present analysis. Figure 1(c) contrasts the shape of an adiabat near the vertex (dashed line) with a normal to the surface (dotted line).

$$\mathbf{r}_u = \mathbf{r}_i + u\hat{\mathbf{n}} \tag{3}$$

where $\hat{\mathbf{n}}$ is the unit vector outward normal to C_i. Taking the derivative of equation (3) with respect to the distance s_i measured along C_i gives (see for example Trim [10])

$$\hat{\mathbf{t}}_u \frac{ds_u}{ds_i} = \hat{\mathbf{t}}_i + u\frac{d\hat{\mathbf{n}}}{ds_i} \tag{4}$$

where $\hat{\mathbf{t}}_i = d\mathbf{r}_i/ds_i$ and $\hat{\mathbf{t}}_u = d\mathbf{r}_u/ds_u$ are the unit tangent vectors along C_i and C_u, respectively. Upon forming the dot product of equation (4) with $\hat{\mathbf{n}}$, and noting that $\hat{\mathbf{t}}_i \cdot \hat{\mathbf{n}} = 0$, we obtain

$$\hat{\mathbf{n}} \cdot \hat{\mathbf{t}}_u \frac{ds_u}{ds_i} = u\hat{\mathbf{n}} \cdot \frac{d\hat{\mathbf{n}}}{ds_i} = \frac{u}{2}\frac{d(\hat{\mathbf{n}} \cdot \hat{\mathbf{n}})}{ds_i}. \tag{5}$$

Since $\hat{\mathbf{n}} \cdot \hat{\mathbf{n}} = 1$, it follows that the derivative on the right hand side of equation (5) is zero, so that equation (5) becomes

$$\hat{\mathbf{n}} \cdot \hat{\mathbf{t}}_u = 0. \tag{6}$$

And since $\hat{\mathbf{n}} \cdot \hat{\mathbf{t}}_i = 0$, it then follows that $\hat{\mathbf{t}}_i = \hat{\mathbf{t}}_u$. Substituting

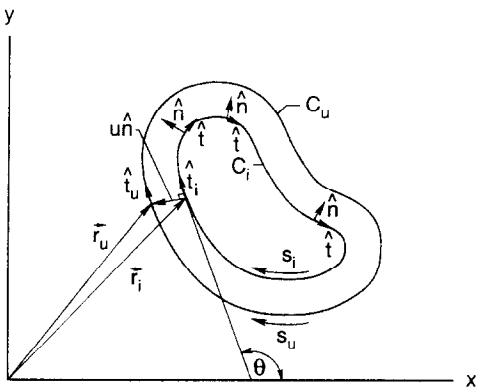

FIG. 2. Vector representation of C_o and C_i used to develop the proof of equation (2).

$\hat{\mathbf{t}}_i = \hat{\mathbf{t}}_u$ in equation (4), forming the equation's dot product with $\hat{\mathbf{t}}_i$, and integrating the resulting equation with respect to ds_i around the whole curve C_i, we obtain

$$P_u = P_i + u\oint_{C_i} \frac{d\hat{\mathbf{n}}}{ds_i} \cdot \hat{\mathbf{t}}_i \, ds_i. \tag{7}$$

According to the third Frenet–Serret formula applied to a planar region

$$d\hat{\mathbf{n}}/ds_i = \frac{d\theta}{ds_i}\hat{t}_i$$

where θ is the angle between $\hat{\mathbf{t}}_i$ and the x-axis, equation (7) reduces to

$$P_u = P_i + u\oint_{C_i} \frac{d\theta}{ds_i} ds_i = P_i + u\oint_{C_i} d\theta, \tag{8}$$

and because for a non-self-intersecting C_i, the tangent vector rotates through exactly 2π radian, regardless of the curve shape, equation (2) follows.

This same equation can be readily derived for the case in which C_i is a polygon of n sides, it being understood that, at the vertices, C_u is completed by constructing arcs, as explained in the Introduction. In this case, one can readily show that P_u and P_i differ by the sum of the lengths of these arcs. Since all these arcs have the radius u, $(P_u - P_i)/u$ is simply the sum of the polygon's external angles minus $n\pi$, and this difference reduces to 2π. Thus equation (2) is valid for polygons as well as for smooth curves, and so it will obviously also be true for curves having both smooth parts and vertices.

Curves C_u as isotherms

Following Elrod's method, we arbitrarily choose the shapes of the isotherms, opting to choose the curves C_u (we leave until later a justification for this particular choice). To assign temperatures to the curves, we note that the resistance dR of the region between curves at u and $u+du$ is given by

$$dR = \frac{du}{klP_u} = \frac{du}{kl(P_i + 2\pi u)} \tag{9}$$

where l is the length measured in the axial direction. This equation follows from the fact that the region is so thin that it has the same thermal resistance as a planar region of the same thickness du and the same heat flow area lP_u. The resistance R_u from $u = 0$ to $u = u$ is obtained by integrating equation (9) to give,

$$R_u = \frac{1}{2\pi lk} \ln\left(1 + \frac{2\pi u}{P_i}\right). \tag{10}$$

The total resistance, R, the quantity of ultimate interest, is

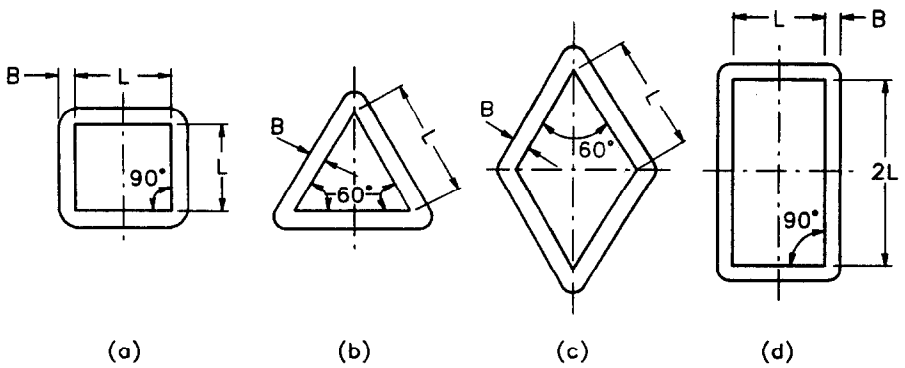

FIG. 3. Several sharp-cornered bodies for which the shape factor was computed by numerically solving the steady heat diffusion equation.

obtained by setting $u = B$ in equation (10):

$$R = \frac{1}{2\pi lk}\ln\left(1+\frac{2\pi B}{P_i}\right). \tag{11}$$

So the shape factor S per unit length l is given by

$$S/l = \frac{2\pi}{\ln\left(1+\frac{2\pi B}{P_i}\right)}. \tag{12}$$

Letting T_u be the temperature at isotherm u, continuity of heat flow Q gives

$$Q = R(T_o - T_i) = R_u(T_u - T_i). \tag{13}$$

From this we obtain the equation that assigns temperatures to the curves:

$$T_u = T_i + (T_o - T_i)\frac{\ln(1+2\pi u/P_i)}{\ln(1+2\pi B/P_i)}. \tag{14}$$

The isotherms chosen in this way have a number of properties in common with the true isotherms. First, they satisfy the boundary conditions and approach (as they should) C_i and C_u in a smooth way as $u \to 0$ and B, respectively. Second, the set of lines everywhere perpendicular to C_u obey many of the necessary properties of the adiabats. For as was shown earlier, the normals to C_u are normal to C_i at $u = 0$ and to C_o at $u = B$ (equation (6)). This means that at all isothermal boundaries, the curves normal to the proposed isotherms are perpendicular to the boundary—a necessary condition for matching the true adiabats.

Indeed, the set C_u and its normals obey so many properties required by the true isotherms and adiabats, that one may wonder whether they are in fact the true isotherms and abiabats. But the one additional condition that must be satisfied (Eckert and Drake [11])—that they must form curvilinear squares in the limit of very finely separated lines—is not satisfied. Deviations of the normals from the true adiabats are most pronounced around vertices. Examination of exact solutions around vertices shows that the true adiabats are curved: starting from a point on C_i near the vertex (Fig. 1(c)), they initially follow the normal to that surface, but then they bend to intersect C_o at the arc part of C_o. The corresponding normals to C_u, on the other hand, are straight everywhere and meet on the flat part of C_o.

Since these differences are most pronounced near any vertices, the error associated with using equation (12) should be greatest when C_i has vertices; moreover, the smaller the vertex angle, the greater should be the error.

TESTING THE MODEL

To evaluate the error in equation (12), we numerically solved Laplace's equation inside the layers shown in Fig. 3. These regions, which are all generated by curves C_i having sharp vertices, are as follows: the square, the equilateral triangle, the 60° rhombus, and the 2:1 rectangle. The calculations covered a range of thickness B (see Table 1).

The finite volume code used to numerically solve Laplace's equation drew from the WATSHARE library of subroutines developed at the University of Waterloo, and used a grid refinement scheme developed by Galpin and Raithby [12]. The accuracy of the resulting code, which has been used in a previous study for three-dimensional bodies (see Hassani and Hollands [13]), was tested by comparing its predictions for S/l with known analytical solutions (e.g. for C_i being a circle); the errors were found to be less than 0.5%. Grid refinement was performed in each case until the difference between successive solutions was less than 0.5%. It was con-

Table 1. Results for cylinders of various cross-sections

	Rhombus			Triangular			Square			Rectangular		
B/L	S/l num.	S/l equation (12)	% diff.	S/l num.	S/l equation (12)	% diff.	S/l num.	S/l equation (12)	% diff.	S/l num.	S/l equation (12)	% diff.
0.10	41.79	43.07	3.0	32.06	33.04	3.0	41.91	43.07	2.8	61.31	63.09	2.9
0.15	29.16	29.69	1.8	22.50	22.99	2.2	28.95	29.69	2.6	41.98	43.06	2.6
0.20	22.64	22.99	1.6	17.64	17.96	1.8	22.43	22.99	2.5	32.23	33.04	2.5
0.40	12.56	12.89	2.6	10.02	10.32	3.0	12.53	12.89	2.5	17.58	17.96	2.2
0.50	10.56	10.83	2.6	8.52	8.77	2.9						
0.60							9.24	9.46	2.4	12.59	12.88	2.3
0.75	7.86	8.07	2.7	6.46	6.65	2.9						
1.00	6.48	6.65	2.6	5.40	5.56	2.9	6.51	6.65	2.2	8.59	8.76	2.0
2.00	4.32	4.42	2.3	3.72	3.82	2.7	4.36	4.42	1.4	5.46	5.56	1.8
3.00	3.58	3.61	0.8	3.12	3.16	1.3	3.60	3.61	0.3	4.37	4.42	1.1

cluded that the difference between the exact value of S/l and the numerically calculated value should be less than about $\pm 1.0\%$.

Comparison between the numerically calculated value of S/l and that given by equation (12) is shown in Table 1. This table shows that the values of S/l given by equation (12) agree with the numerically calculated ones to within a maximum error of 3%. Part of this 3% error is attributable to the errors in the computational scheme; the randomness of this type of error accounts for the fact that the error changes with B/L ratio as shown in Table 1. As shown by Elrod [9], an arbitrary selection of the location of the isotherms produces an upper bound for the shape factor, and these calculations have borne this out: the results from equation (12) are always higher than the results produced numerically. On the other hand, the assumed locations of the isotherms appear to be close enough to the true isotherms, because the maximum difference between the predicted results and the numerical results in this work is only 3%. Since these results are for bodies having sharp vertices, equation (12) should be even more precise for smooth bodies. Thus it would appear that equation (12) yields results suitable for most engineering calculations.

REFERENCES

1. G. D. Raithby and K. G. T. Hollands, *Handbook of Heat Transfer Fundamentals* (Edited by W. M. Rohsenow, J. P. Hartnett and E. N. Ganic) (2nd Edn) Chap. 6. McGraw-Hill, New York (1985).
2. J. C. Smith, J. E. Lind and D. S. Lermand, Shape factors for conductive heat flow, *A.I.Ch.E. Jl* 330–331 (1958).
3. M. J. Balcerzak and S. Rayner, Steady state temperature distribution and heat flow in prismatic bars with isothermal boundary conditions, *Int. J. Heat Mass Transfer* **3,** 113–125 (1961).
4. G. K. Lewis, Shape factors in conduction heat flow for circular bars and slabs with various internal geometries, *Int. J. Heat Mass Transfer* **11,** 985–992 (1968).
5. J. P. Dugan, On the shape factor for a hollow, square cylinder, *Am. Inst. Chem. Engs J.* **18**(5), 1082–1083 (1972).
6. P. A. A. Laura and E. A. Susemihl, Determination of heat flow shape factors for hollow, regular polygonal prisms, *Nuclear Engng and Design* **25,** 409–412 (1973).
7. P. A. A. Laura and G. Sanchez Sarmiento, Heat flow shape factors for circular rods with regular polygonal concentric inner bore, *Nuclear Engng and Design* **47,** 227–229 (1978).
8. L. M. Simeza and M. M. Yovanovich, Shape factors for hollow prismatic cylinders bounded by isothermal inner circles and outer regular polygons, *Int. J. Heat Mass Transfer* **30,** 812–816 (1987).
9. H. G. Elrod, Two simple theorems for establishing bounds on the total heat flow in steady-state heat conduction problems with convective boundary conditions, *J. Heat Transfer* 65–70 (1974).
10. D. W. Trim, *Calculus and Analytic Geometry*. Addison-Wesley, Reading, MA (1983).
11. E. R. G. Eckert and R. M. Drake, *Analysis of Heat and Mass Transfer*. McGraw-Hill, New York (1972).
12. P. Galpin and G. D. Raithby, Personnal communications, 1988.
13. A. V. Hassani and K. G. T. Hollands, Conduction shape factor for a region of uniform thickness surrounding a three-dimensional body of arbitrary shape, *J. Heat Transfer* **112,** 492–495 (1990).
14. P. A. A. Laura and G. Sanchez Sarmiento, Analytical determination of heat flow shape factors for composite, prismatic bars of doubly-connected cross section, *Nuclear Engng and Design* **50,** 397–385 (1978).